JACS
JOURNAL OF THE AMERICAN CHEMICAL SOCIETY

COMMUNICATION

pubs.acs.org/JACS

Diffusion-Controlled Luminescence Quenching in Metal−Organic Frameworks

Cheng Wang and Wenbin Lin*

Department of Chemistry, CB#3290, University of North Carolina, Chapel Hill, North Carolina 27599, United States

Supporting Information

ABSTRACT: Diffusion-controlled luminescence quenching of a phosphorescent metal−organic framework built from the $Ru(bpy)_3^{2+}$-derived bridging ligand (MOF-**1**) was studied using a series of amines of different sizes as quenchers. The dynamics of amine diffusion into solvent-filled MOF-**1** channels was probed by modeling time-dependent luminescence quenching data, which provide quantitative diffusion coefficients for the amine quenchers. Triethylamine, tripropylamine, and tributylamine were found to follow Fickian diffusion with a diffusivity of $(1.1 \pm 0.2) \times 10^{-13}$, $(4.8 \pm 1.2) \times 10^{-14}$, and $(4.0 \pm 0.4) \times 10^{-14}$ m^2/s, respectively. Diisopropylethylamine (DIPEA), on the other hand, was found to be too large to enter the MOF channels. Despite its size, 4-MeOPhNPh$_2$ can enter the MOF channels via a slow, complicated framework/guest intercalation process to result in extensive framework distortion as revealed by powder X-ray diffraction. This work represents the first quantitative study of the dynamics of molecular diffusion into solvent-filled MOF channels. Such quantitative information on molecular diffusion in MOFs is of fundamental importance to many of their potential applications (e.g., heterogeneous catalysis).

Metal−organic frameworks (MOFs), constructed from a variety of molecular linkers and metal or metal cluster connecting points, have emerged as a new class of molecularly tunable porous solids.[1−5] While the application of MOFs in gas storage and separation has been extensively explored in the past decade,[6−8] other important areas such as liquid-phase separation,[9,10] drug delivery,[11,12] chemical sensing,[13−16] biomedical imaging,[17,18] and particularly selective catalysis of various organic transformations[19−23] have started to attract interest recently. In many of these applications, mass transport properties of MOFs play a dominant role on their performances. Diffusion coefficient (or diffusivity) of MOFs, a key parameter characterizing the transport process, is thus an important physical quantity to be determined.

Guest molecule diffusivity in MOFs was first computationally studied using molecular dynamics (MD) simulations. Sarkisov et al. first reported theoretical predictions of self-diffusion coefficient D_s of several alkanes in MOF-**5**.[24] Sholl, Johnson, Schmid, and others also examined self-diffusion coefficient D_s and transport diffusion coefficient D_t of simple alkanes, hydrogen, carbon dioxide, benzene, and other small molecules in several MOFs including the IRMOF series and HKUST-**1**.[25−29]

In contrast to a wealth of literature on simulation efforts, there are only a few published experimental studies of measuring diffusivity in MOFs. Stallmach et al. first reported self-diffusivity of hydrocarbons in MOF-**5**,[30] and more recently in HKUST-**1**,[31] using the pulsed-field gradient NMR technique. Jobic and Maurin used quasi-elastic neutron scattering method to study self-diffusion of H_2, CO_2, and alkanes in MIL-47(V) and MIL-53(Cr).[32−35] In another direction, Kärger and co-workers used interference microscopy[36] and infrared microscopy[37] to study respectively transport diffusion of methanol into vacuum-activated manganese formate and alkanes into vacuum-activated HKUST-**1**. Quartz crystal microbalance measurement of thin films was also employed by Zybaylo et al. to estimate the diffusivity of pyridine in vacuum-activated HKUST-**1**.[38]

These measurements provide invaluable information for the applications of MOFs in gas-phase adsorption and separation. However, many of interesting applications of MOFs, such as heterogeneous catalysis, involve liquid suspensions of MOFs. In these cases, diffusion occurs when MOF channels are already filled with solvent molecules. The realistic physical picture involves continuous exchange of diffusant molecules (e.g., substrate or product molecules in MOF catalysis) with solvent molecules during their transport through MOF channels, instead of self-diffusion or transport diffusion into vacuum-activated MOFs. This kind of diffusion process is expected to be much slower than self-diffusion or transport diffusion. There were two studies on molecular diffusion into solvent-filled MOF channels,[39,40] but quantitative diffusivities could not be determined in these experiments.

In our exploration of photoactive MOFs, we encountered an interesting diffusion-controlled quenching phenomenon, in which amine quenchers in solution diffuse into MOF channels and gradually quench the MOF emission from the $Ru(bpy)_3^{2+}$-derived bridging ligand via a redox quenching mechanism.[41] We proposed that such time-dependent luminescence quenching behaviors can be utilized to model the diffusion processes of different quenchers in MOFs in solution. In a related study, diffusion coefficients of fluorescein in lysozyme crystals were obtained by modeling the fluorescence intensities determined by confocal laser scanning microscopy.[42]

The phosphorescent MOF (**1**) used in this study contains a $Ru(bpy)_3^{2+}$ derivative H_2**L**, which was synthesized by directly reacting *cis*-$[Ru(bpy)_2Cl_2]$ with 2,2′-bipyridine-5,5′-dicarboxylate

Received: December 12, 2010
Published: March 08, 2011

Scheme 1. Synthesis of Phosphorescent MOF-1 and Chemical Structures of Amine Quenchers of Varying Sizes

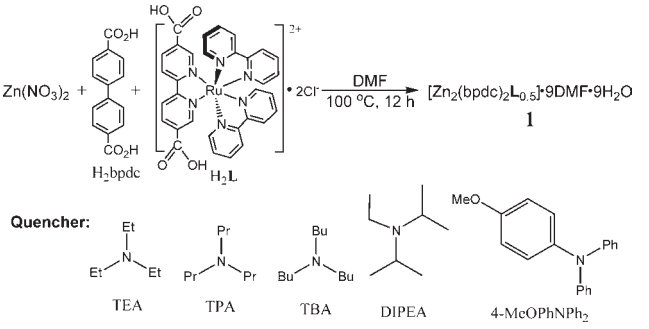

acid.[43] H_2**L** was mixed with 4,4′-biphenyldicarboxylic acid (H_2BPDC) and then reacted with $Zn(NO_3)_2 \cdot 6H_2O$ in DMF at 100 °C for 12 h to obtain yellow-red crystals with thin-plate or feather-like morphologies (Scheme 1).

1 crystallizes in the orthorhombic $C222_1$ space group, as revealed by a single-crystal X-ray diffraction study. The three-dimensional (3D) framework of **1** is built from linking $[Zn_2(\mu_2\text{-}CO_2)_3]$ SBUs with ditopic BPDC and **L** bridging ligands (Figure 1a). The asymmetric unit of **1** contains 5/2 of the dicarboxylate ligands (2 BPDC and 0.5 **L** ligands) and one Zn_2 SBU (Figure 1b). The **L** and BPDC ligands are found to randomly occupy two of the three independent ligand positions (see Supporting Information [SI] for detailed treatment of occupancy disorder), with the third ligand position exclusively occupied by the BPDC ligand. Such an occupancy disorder precludes precise determination of the **L**/BPDC ratio by X-ray crystallography. Instead, the Ru complex content **L**/(BPDC + **L**) in **1** was determined by quantitative UV−vis spectroscopy and ICP-MS to be 20%, leading to a framework formula of $Zn_2\mathbf{L}_{0.5}(BPDC)_2$ for **1**.

Three bidentate carboxylate groups bridge the two Zn atoms in the equatorial positions of the Zn_2 SBU, and the tetrahedral coordination environment of each Zn center is completed by a monodentate carboxylate group in the axial positions of the Zn_2 SBU. The Zn_2 SBUs are thus connected to each other by five dicarboxylate ligands to form a 3D framework of five-connected **bnn** topology (Figure 1c) that exhibits enormous void space (Figures S4.1 and S4.2 [SI]) and readily accommodates a second framework via interpenetration, leading to a two-fold interpenetrating structure for **1**. Even with two-fold interpenetration, **1** exhibits large open channels that are filled with solvent molecules. A combination of TGA and ^{1}H NMR analysis affords the complete formula of $[Zn_2\mathbf{L}_{0.5}(BPDC)_2] \cdot 9DMF \cdot 9H_2O$ for **1**. As a result of disordered nature of the **L** ligands in the frameworks, the open channel sizes along the [001] direction vary from 0.4 nm × 0.7 nm to 0.9 nm ×1.2 nm (Figure 1a).

Luminescence quenching experiments were performed on plate-like single crystals of **1** affixed to the bottom of a quartz fluorescent cuvette, with faces perpendicular to the cuvette bottom and immersed in cyclohexane (Scheme 2). The original DMF/H_2O solvent molecules inside the channels of **1** were first exchanged with CH_2Cl_2 and then with cyclohexane. The O_2 molecules inside the channels were removed by keeping the crystal in degassed cyclohexane overnight to prevent the luminescence quenching by O_2 via an energy-transfer pathway. The thicknesses of plate-like crystals of **1** were measured using a

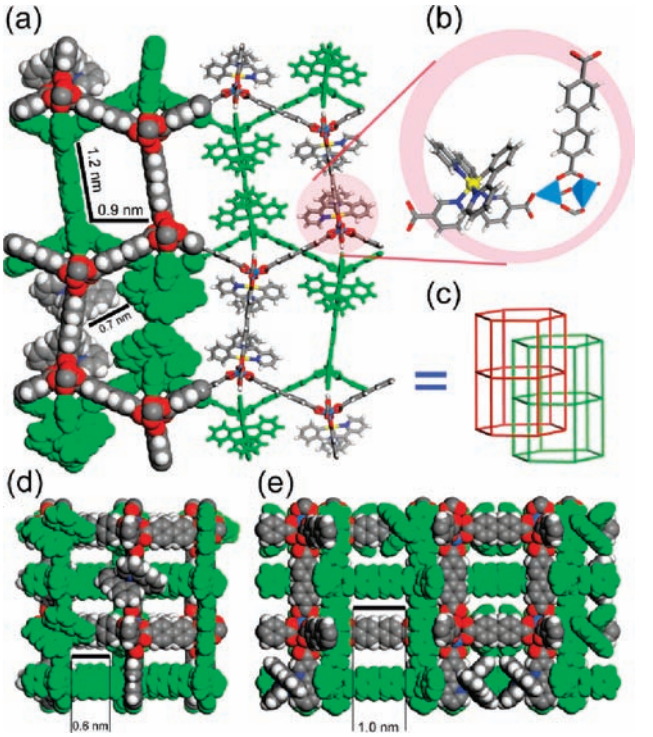

Figure 1. Structure model of MOF-**1**. (a) Space-filling and stick model viewed along the [001] direction, showing different channel sizes due to different local distributions of **L** ligands. (b) Building blocks of **1**. (c) Schematic showing two-fold interpenetrating frameworks of the **bnn** topology. (d) Space-filling model viewed along the [100] direction. (e) Space-filling model viewed along the [010] direction.

Scheme 2. Schematic of the Experimental Setup Used for Luminescence Quenching Measurements

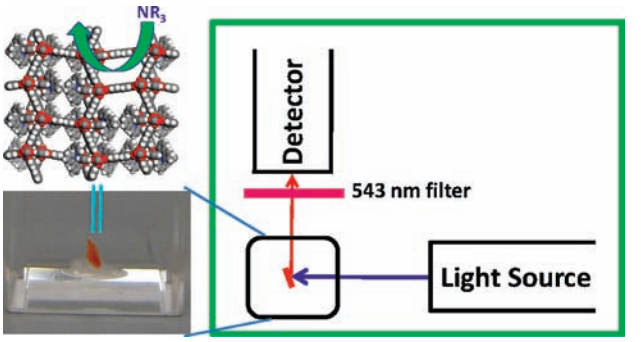

microscope with a built-in ruler. In the quenching experiment, a MOF-**1** crystal was excited at a wavelength of 452 nm, and the emission intensity at 627 nm was recorded at different time points after the addition of a predetermined amount of amine quenchers. The amines or solutions of amines were fully degassed before use. Structures of the amines are shown in Scheme 1. Excitation light was blocked from impinging on the crystal during the intervals between different emission measurements to avoid photodecomposition of the amine and other irreversible photochemical processes. A typical emission measurement took about 2 to 3 s, during which time the crystal and quenchers were exposed to light. The average value of the emission signals was recorded, and the experimental error for

dx.doi.org/10.1021/ja111197d |J. Am. Chem. Soc. 2011, 133, 4232–4235

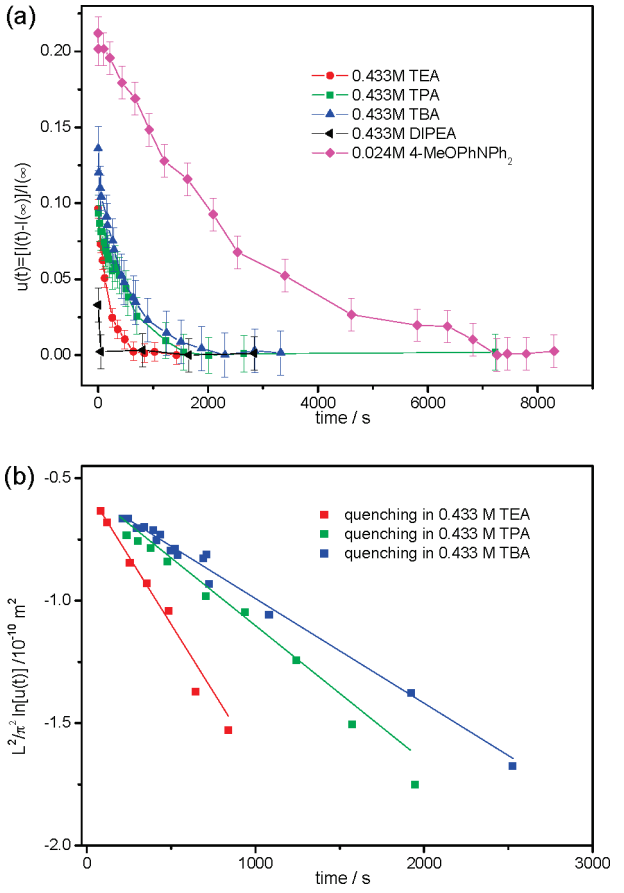

Figure 2. (a) Plots of $u(t) = [I(t) - I(\infty)]/I(\infty)$ vs t for different amine quenchers: TEA (red), TPA (green), TBA (blue), DIPEA (black), and 4-MeOPhNPh$_2$ (purple) (see SI for more detailed plots). (b) Linear fitting of $(L^2/\pi^2)\ \ln[u(t)]$ vs t of TEA (red), TPA (green), and TBA (blue). Only the data points of $t > 100$ s for TEA and $t > 200$ s for TPA and TBA were used in these fits (see SI for more detailed analyses).

each time point was estimated from the signal fluctuations within the 2 to 3 s. Spectra of the crystals were taken before and after the quenching studies to ensure that no substantial spectra change had occurred (Figure S6.1 [SI]).

The time-dependent intensity $I(t)$ was normalized against the equilibrium intensity after a long time $I(\infty)$. A plot of $u(t) = [I(t) - I(\infty)]/I(\infty)$ vs time is shown in Figure 2a. Exponential decay of the emission intensities over time to 80−85% of their initial values was observed in solutions of 0.433 M triethylamine (TEA), tripropylamine (TPA), tributylamine (TBA), and 0.024 M 4-methoxylphenyldiphenylamine (4-MeOPhNPh$_2$) as a result of diffusion-controlled luminescence quenching of **1** by these amines. The amount of time required for the emission to reach equilibrium after adding TEA, TPA, TBA, and 4-MeOPhNPh$_2$ is approximately 10, 30, 30, and 120 min, respectively. This order of increase in time required to reach equilibrium correlates well with the sizes of these amines.

For diisopropylethylamine (DIPEA) quenching, however, the intensity dropped instantaneously to 96% of its original value and remained unchanged after that. This behavior is likely a result of surface quenching only, suggesting that DIPEA cannot enter the MOF channels. To confirm this, we investigated the reverse process of amine diffusing out of the MOF channels. Crystals fully soaked in amine solutions were put back into freshly degassed cyclohexane under N_2 protection, and the changes in emission intensities were monitored. An increase of signal over time was observed for TPA- and 4-MeOPhNPh$_2$-treated MOFs, indicating the release of absorbed quenchers. In contrast, for the MOFs soaked in DIPEA, no signal increase was detected. This result supports the notion that no DIPEA can enter in MOF channels, presumably owing to its large size (Figure S7.1 [SI]). Further evidence comes from GC analysis of the absorbed amine in the MOF channels. Amine-treated **1** released substantial amounts of TPA, TBA, and 4-MeOPhNPh$_2$, but no DIPEA (SI). These results unambiguously prove the accessibility of the MOF channels to all the amines except DIPEA.

Geometry-optimized structure of 4-MeOPhNPh$_2$ is much larger than that of DIPEA (SI), so their different uptake behaviors by **1** cannot be explained simply based on their sizes. Instead, we believe that different uptake behaviors of the two amines stem from their disparate affinities toward the MOF channels. 4-MeOPhNPh$_2$, as an aromatic amine, can strongly interact with the MOF channel wall via $\pi-\pi$ interactions, whereas aliphatic chains of DIPEA do not provide such a driving force for inclusion. PXRD patterns of amine-treated crystals of **1** were taken to provide insights into these different uptake behaviors. While the PXRD patterns of all the aliphatic amine-treated MOFs closely resemble that of the as-synthesized **1**, the pattern of 4-MeOPhNPh$_2$−treated MOF crystals lose all of the diffraction peaks due to **1** (Figure S9.1 [SI]). The severe framework structure distortion of 4-MeOPhNPh$_2$-treated **1** suggests that 4-MeOPhNPh$_2$ enters the MOF by intercalating into the framework via $\pi-\pi$ interactions instead of simple Fickian diffusion.

We quantitatively analyze the diffusion of TEA, TPA, and TBA in the framework of Fickian diffusion. In other words, we assume a constant diffusivity, D, independent of local concentration of amine quenchers. By taking advantage of thin-plate morphology of the MOF crystals, we further simplify the diffusion process into a 1D diffusion described by Fick's second law (Eq 1) with the boundary conditions and initial conditions expressed in Eq 2 and Eq 3, respectively:

$$\frac{\partial c(x,t)}{\partial t} = D\frac{\partial^2 c(x,t)}{\partial x^2} \qquad \text{(Eq 1)}$$

$$c(0,t) = c(L,t) = c_0 \qquad \text{(Eq 2)}$$

$$c(x,0) = 0 (0 < x < L) \qquad \text{(Eq 3)}$$

For the emission quenching, we assume a rapid, reversible quenching behavior that can be described by the Stern−Volmer equation. In addition, activity correction for amine concentration inside MOF channels, the sample dependent crystal geometry and position factor, and the contribution from surface emission have also been considered. Using this model, the time-dependent normalized emission intensity was derived (SI), and can be expressed with Eq 4:

$$u(t) \approx A\exp\left(-\left[\pi^2 Dt\right]/L^2\right) \qquad \text{(Eq 4)}$$

where A is independent of time t and is expressed by $A = (1/(1 + \delta))\ ([4\alpha\beta c_0]/[1 + \alpha\beta c_0])\ ([\in L]/[\cos\theta])/([(\in L)/(\cos\theta)]^2 + \pi^2)$ (α, β, $\in$, θ, and δ are introduced to account for Stern−Volmer quenching, activity correction, crystal absorption, crystal positioning, and surface emission, respectively, see SI); L is thickness of the crystal, and D is the Fickian diffusivity.

dx.doi.org/10.1021/ja111197d |J. Am. Chem. Soc. 2011, 133, 4232–4235

Plots of $(L^2/\pi^2)\ln[u(t)]$ vs t gave straight lines (Figure 2b), indicating the validity of the Fickian diffusion model as described by Eq 4. Diffusivities of TEA, TPA, and TBA in MOF-**1** could be obtained from the slopes of these linear fits, and were determined to be $(1.1 \pm 0.2) \times 10^{-13}$, $(4.8 \pm 1.2) \times 10^{-14}$, and $(4.0 \pm 0.4) \times 10^{-14}$ m^2/s, respectively. These values are 1−2 orders of magnitude smaller than the transport diffusivity reported for methanol into vacuum-activated porous manganese formate crystals,[36] a system that has a similar diffusant/channel size ratio as our present case. This discrepancy is expected since the two diffusion processes are of very different natures. The diffusivity derived in our present study is much more relevant to many applications that involve liquid suspensions of MOFs.

In summary, we have examined diffusion-controlled luminescence quenching of a $Ru(bpy)_3^{2+}$-incorporated MOF by a series of amines of different sizes. TEA, TPA, and TBA can diffuse through the MOF channels according to the time-dependent quenching data, whereas DIPEA is too large to enter the MOF channels. Despite its large size, 4-MeOPhNPh$_2$ can enter the MOF channels via a slow, complicated framework/guest intercalation process to result in extensive framework distortion as revealed by PXRD. The time-dependent quenching curves of TEA, TPA, and TBA were fitted quantitatively with a 1D Fickian diffusion model to afford diffusivities on the order of 10^{-14}−10^{-13} m^2/s. These diffusivities are 1−2 orders of magnitude smaller than that of a transport diffusion system of a similar diffusant/channel size ratio. The dynamics of molecular diffusion into solvent-filled MOF channels reported herein is of fundamental importance to many MOF applications in solution.

■ ASSOCIATED CONTENT

Supporting Information. Experimental procedures, characterization data, detailed derivations of the diffusion equations, and complete ref 11. This material is available free of charge via the Internet at http://pubs.acs.org.

■ AUTHOR INFORMATION

Corresponding Author
wlin@unc.edu

■ ACKNOWLEDGMENT

We acknowledge financial support from NSF. We made use of the UNC EFRC instrumentation facility which is funded jointly by the U.S. Department of Energy Office of Science (BES, DE-SC0001011) and Office of Energy Efficiency & Renewable Energy (DE-EE0003188).

■ REFERENCES

(1) Bradshaw, D.; Warren, J. E.; Rosseinsky, M. J. *Science* **2007**, *315*, 977.
(2) Evans, O. R.; Lin, W. *Acc. Chem. Res.* **2002**, *35*, 511.
(3) Ferey, G.; Mellot-Draznieks, C.; Serre, C.; Millange, F. *Acc. Chem. Res.* **2005**, *38*, 217.
(4) Kitagawa, S.; Kitaura, R.; Noro, S. *Angew. Chem., Int. Ed.* **2004**, *43*, 2334.
(5) Ockwig, N. W.; Delgado-Friedrichs, O.; O'Keeffe, M.; Yaghi, O. M. *Acc. Chem. Res.* **2005**, *38*, 176.
(6) Li, J. R.; Kuppler, R. J.; Zhou, H. C. *Chem. Soc. Rev.* **2009**, *38*, 1477.
(7) Pan, L.; Olson, D. H.; Ciemnolonski, L. R.; Heddy, R.; Li, J. *Angew. Chem., Int. Ed.* **2006**, *45*, 616.
(8) Ma, L.; Mihalcik, D. J.; Lin, W. *J. Am. Chem. Soc.* **2009**, *131*, 4610.
(9) Alaerts, L.; Maes, M.; Giebeler, L.; Jacobs, P. A.; Martens, J. A.; Denayer, J. F. M.; Kirschhock, C. E. A.; De Vos, D. E. *J. Am. Chem. Soc.* **2008**, *130*, 14170.
(10) Maes, M.; Alaerts, L.; Vermoortele, F.; Ameloot, R.; Couck, S.; Finsy, V.; Denayer, J. F. M.; De Vos, D. E. *J. Am. Chem. Soc.* **2010**, *132*, 2284.
(11) Horcajada, P.; et al. *Nat. Mater.* **2010**, *9*, 172.
(12) Rieter, W. J.; Pott, K. M.; Taylor, K. M.; Lin, W. *J. Am. Chem. Soc.* **2008**, *130*, 11584.
(13) Allendorf, M. D.; Houk, R. J.; Andruszkiewicz, L.; Talin, A. A.; Pikarsky, J.; Choudhury, A.; Gall, K. A.; Hesketh, P. J. *J. Am. Chem. Soc.* **2008**, *130*, 14404.
(14) Chen, B.; Wang, L.; Xiao, Y.; Fronczek, F. R.; Xue, M.; Cui, Y.; Qian, G. *Angew. Chem., Int. Ed.* **2009**, *48*, 500.
(15) Lan, A.; Li, K.; Wu, H.; Olson, D. H.; Emge, T. J.; Ki, W.; Hong, M.; Li, J. *Angew. Chem., Int. Ed.* **2009**, *48*, 2334.
(16) Xie, Z.; Ma, L.; deKrafft, K. E.; Jin, A.; Lin, W. *J. Am. Chem. Soc.* **2010**, *132*, 922.
(17) deKrafft, K. E.; Xie, Z.; Cao, G.; Tran, S.; Ma, L.; Zhou, O. Z.; Lin, W. *Angew. Chem., Int. Ed.* **2009**, *48*, 9901.
(18) Lin, W.; Rieter, W. J.; Taylor, K. M. *Angew. Chem., Int. Ed.* **2009**, *48*, 650.
(19) Lee, J.; Farha, O. K.; Roberts, J.; Scheidt, K. A.; Nguyen, S. T.; Hupp, J. T. *Chem. Soc. Rev.* **2009**, *38*, 1450.
(20) Lin, W. B. *MRS Bull.* **2007**, *32*, 544.
(21) Ma, L.; Abney, C.; Lin, W. *Chem. Soc. Rev.* **2009**, *38*, 1248.
(22) Ma, L.; Falkowski, J. M.; Abney, C.; Lin, W. *Nat. Chem.* **2010**, *2*, 838.
(23) Song, F.; Wang, C.; Falkowski, J. M.; Ma, L.; Lin, W. *J. Am. Chem. Soc.* **2010**, *132*, 15390.
(24) Sarkisov, L.; D., T.; Snurr, Q. R. *Mol. Phys.* **2004**, *102*, 211.
(25) Amirjalayer, S.; Schmid, R. *Microporous Mesoporous Mater.* **2009**, *125*, 90.
(26) Amirjalayer, S.; Tafipolsky, M.; Schmid, R. *Angew. Chem., Int. Ed.* **2007**, *46*, 463.
(27) Keskin, S.; Sholl, D. S. *Langmuir* **2009**, *25*, 11786.
(28) Seehamart, K.; Nanok, T.; Karger, J.; Chmelik, C.; Krishna, R.; Fritzsche, S. *Microporous Mesoporous Mater.* **2010**, *130*, 92.
(29) Skoulidas, A. I.; Sholl, D. S. *J. Phys. Chem. B* **2005**, *109*, 15760.
(30) Stallmach, F.; Groger, S.; Kunzel, V.; Karger, J.; Yaghi, O. M.; Hesse, M.; Muller, U. *Angew. Chem., Int. Ed.* **2006**, *45*, 2123.
(31) Wehring, M.; Gascon, J.; Dubbeldam, D.; Kapteijn, F.; Snurr, R. Q.; Stallmach, F. *J. Phys. Chem. C* **2010**, *114*, 10527.
(32) Jobic, H.; Rosenbach, N.; Ghoufi, A.; Kolokolov, D. I.; Yot, P. G.; Devic, T.; Serre, C.; Ferey, G.; Maurin, G. *Chem.—Eur. J.* **2010**, *16*, 10337.
(33) Rosenbach, N.; Jobic, H.; Ghoufi, A.; Salles, F.; Maurin, G.; Bourrelly, S.; Llewellyn, P. L.; Devic, T.; Serre, C.; Ferey, G. *Angew. Chem., Int. Ed.* **2008**, *47*, 6611.
(34) Salles, F.; Jobic, H.; Ghoufi, A.; Llewellyn, P. L.; Serre, C.; Bourrelly, S.; Ferey, G.; Maurin, G. *Angew. Chem., Int. Ed.* **2009**, *48*, 8335.
(35) Salles, F.; Jobic, H.; Maurin, G.; Koza, M. M.; Llewellyn, P. L.; Devic, T.; Serre, C.; Ferey, G. *Phys. Rev. Lett.* **2008**, 100.
(36) Kortunov, P. V.; Heinke, L.; Arnold, M.; Nedellec, Y.; Jones, D. J.; Caro, J.; Karger, J. *J. Am. Chem. Soc.* **2007**, *129*, 8041.
(37) Chmelik, C.; Karger, J.; Wiebcke, M.; Caro, J.; van Baten, J. M.; Krishna, R. *Microporous Mesoporous Mater.* **2009**, *117*, 22.
(38) Zybaylo, O.; Shekhah, O.; Wang, H.; Tafipolsky, M.; Schmid, R.; Johannsmann, D.; Woll, C. *Phys. Chem. Chem. Phys.* **2010**, *12*, 8092.
(39) Choi, H. J.; Suh, M. P. *J. Am. Chem. Soc.* **2004**, *126*, 15844.
(40) Han, S. B.; Wei, Y. H.; Valente, C.; Lagzi, I.; Gassensmith, J. J.; Coskun, A.; Stoddart, J. F.; Grzybowski, B. A. *J. Am. Chem. Soc.* **2010**, *132*, 16358.
(41) Kalyanasundaram, K. *Coord. Chem. Rev.* **1982**, *46*, 159.
(42) Cvetkovic, A.; Picioreanu, C.; Straathof, A. J. J.; Krishna, R.; van der Wielent, L. A. M. *J. Am. Chem. Soc.* **2005**, *127*, 875.
(43) Xie, P. H.; Hou, Y. J.; Zhang, B. W.; Cao, Y.; Wu, F.; Tian, W. J.; Shen, J. C. *J. Chem. Soc., Dalton Trans.* **1999**, 4217.